The presence of pyruvate carboxylase in the human brain and its role in the survival of cultured human astrocytes

Eduard Gondáš[1, 2], Alžbeta Kráľová Trančíková[2,3], Jakub Šofranko[1],Petra Majerová[3], Vincent Lučanský[2], Matúš Dohál[2], Andrej Kováč[3], Radovan Murín[1*]

[1] Department of Medical Biochemistry, Jessenius Faculty of Medicine in Martin, Comenius University Bratislava, Slovakia

[2] Biomedical Center Martin, Jessenius Faculty of Medicine in Martin, Comenius University Bratislava, Martin, Slovakia

[3] Institute of Neuroimmunology of SAS, Bratislava, Slovakia

Correspondence to: Radovan Murín, Department of Medical Biochemistry, Jessenius Faculty of Medicine in Martin, Comenius University in Bratislava, 036 01 Martin, Slovakia

E-mail: murin@jfmed.uniba.sk

Abstract

Pyruvate carboxylase (PC) is a mitochondrial, biotin-containing enzyme catalyzing the ATP-dependent synthesis of oxaloacetate from pyruvate and bicarbonate, with a critical anaplerotic role in sustaining the brain metabolism. Based on the studies performed on animal models, PC expression was assigned to be glia-specific. To study PC distribution among human neural cells, we probed the cultured human astrocytes and brain sections with antibodies against PC. Additionally, we tested the importance of PC for the viability of cultured human astrocytes by applying the PC inhibitor 3-chloropropane-1,2-diol (CPD). Our results establish the expression of PC in mitochondria of human astrocytes in culture and brain tissue and also into a subpopulation of the neurons *in situ*. CPD negatively affected the viability of astrocytes in culture, which could be partially reversed by supplementing media with malate, 2-oxoglutarate, citrate, or pyruvate. The provided data estimates PC expression in human astrocytes and neurons in human brain parenchyma. Furthermore, the enzymatic activity of PC is vital for sustaining the viability of cultured astrocytes.

Keywords: pyruvate carboxylase, brain, astrocyte, neuron, anaplerotic metabolism

Introduction

Brain metabolism relies on importing substrates from the bloodstream through the blood-brain barrier (BBB). The restricted transporting capability of the BBB for several biomolecules, *e.g.*, lipids and glutamate, is considered to be compensated by the synthetic ability of brain cells to support the demand for them. In this respect, brain cells withdraw some intermediates from the TCA cycle and use them as substrates for biosynthetic reactions [1]. The anaplerotic process should compensate for the loss of the intermediates in the TCA cycle to prevent the collapse of mitochondrial metabolism [2–4]. Among the possible anaplerotic strategies, the enzymatic conversion of pyruvate to oxaloacetate by pyruvate carboxylase (PC) is considered the most prominent in brain parenchyma. Indeed, the importance of PC for sustaining the brain's physiological functions could be stressed by the fact that the patients with PC deficiency (OMIM #266150) exert metabolic disturbances, severe neurological signs, and neuroanatomical alterations [5–9, 9–12].

Pyruvate carboxylase [pyruvate:carbon-dioxide ligase (ADP-forming); EC 6.4.1.1] is a mitochondrial, biotin-containing enzyme that catalyzes the ATP-dependent extension of the pyruvate-carbon skeleton to oxaloacetate. The generation of oxaloacetate in the mitochondrial matrix allows its direct integration into the pool of the TCA cycle intermediates. Considering the importing capacity of BBB for different compounds from the bloodstream [13], glucose is a compound with an import into the brain parenchyma that exceeds all others. In this respect, glucose is a primary source of carbon atoms for synthesizing a plethora of compounds. Their synthesis relies on the withdrawal of the intermediates from the TCA cycle, including neurotransmitters such as glutamate [14]. Therefore, the pyruvate generated by the conversion of glucose in the process of glycolysis [15] can enter the TCA cycle by two major routes: i) either by oxidative decarboxylation to acetyl-CoA by pyruvate dehydrogenase, or ii) by carboxylation to oxaloacetate facilitated by PC [16].

Results of the experiments performed on the rodent models revealed the localization of PC in brain astrocytes [17, 18] and cultured astroglia [19], oligodendroglia [20, 21], microglial, and ependymal cells [20]. Together with the absence of both positive immunocytochemical signal and PC activity (Yu et al. 1983) in cultured neuronal

cells, these lead to postulating the hypothesis about the glia-specific expression of PC. In contrast to this generally accepted view, the results of the experiments based on the estimation of pyruvate carboxylase activity in different brain fractions [22] and cultured neuronal cells point to the hypothesis that also neurons might possess the capability to carboxylate pyruvate [23].

To evaluate a hypothesis about the glia-specific expression of PC among neural cells, we tested the presence of PC among cultured human astrocytes and brain tissue sections. Furthermore, we evaluated to which extent the survival of cultured human astrocytes may be affected by the inhibition of PC. Obtained results show that PC is expressed in human astrocytes either in culture or *in situ* and among a subpopulation of neurons in the human brain. Furthermore, PC activity is vital to sustaining the viability of astrocytes, and metabolites from the TCA cycle could reduce the cytotoxic effect caused by PC inhibition.

Materials and Methods

Cell cultures

All tested human types of cells were obtained from commercial sources and incubated under the recommended conditions. Briefly, the human astrocytic cell line K1884 (N7805-100) was obtained from Gibco, and normal human astrocytes (NHA; ATCC-BXS0117) were purchased from Lonza. The both cell lines were cultured in Dulbecco's modified Eagle medium (DMEM; Gibco) supplemented with 10 % (v/v) fetal bovine serum (FBS; Gibco), 1 % (v/v) N-2 supplement (Gibco), penicillin (100 U/ml) and streptomycin sulphate (0.1 mg/ml). The cells were incubated in a humidified incubator in an atmosphere enriched with 5 % CO_2 at 37 °C. The plastic culture dishes and plates were from Sigma.

Immunoblotting analysis

The cells in culture dish were rinsed with ice-cold phosphate-buffered saline (DPBS, Sigma) for three times and immediately lysed in lysis buffer (15 mM Tris-HCl pH = 7.6, 150 mM NaCl, 1 % (w/w) 3-[(3-cholamidopropyl) dimethylammonio]-1-propane sulfonate, 1 % (v/w) protease inhibitor cocktail). After lysis, the cell lysates were centrifugated at 10,000 × *g*, 4 °C, 5 min, and supernatants were used for protein estimation by Bradford´s method [24]. The same amount of proteins was used for immunoblotting analysis. The proteins (20 µg/lane) were separated in 8 % acrylamide gels by the SDS-PAGE method and immediately used for the electroblotting on the nitrocellulose membrane (Bio-Rad Laboratories). After the electroblotting membrane was blocked with Tris-buffered saline (TBS) supplemented with 0.08 % (w/v) Tween-20 (TBS-T) and 2 mg/ml bovine serum albumin (BSA, AppliChem) for one hour at room temperature (RT). The presence of pyruvate carboxylase among the separated proteins was detected by incubation the membrane with the rabbit antiserum diluted 1:500 in TBS-T with 2 mg/ml BSA at 4 °C for 12 h, followed by the incubation with affinity-purified anti-rabbit IgG conjugated with horse-radish peroxidase (HRP). Generated chemiluminescent signal was initiated by the addition of the SuperSignal West Pico Chemiluminescent Substrate solution (Thermo-Scientific) and recorded by the Chemidoc XRS system (Bio-Rad Laboratories). Immediately the membranes

were stripped and re-stained with mouse monoclonal anti-GAPDH antibodies, followed by incubation with affinity-purified anti-mouse IgG molecules conjugated with HRP. The obtained chemiluminescent signals were processed with the Image Studio™ software (LI-COR Inc.).

Immunofluorescent triple staining of cultured cells

The cells were grown in the Petri dishes with attached sterile glass coverslips at the bottom under the standard culture procedure to approximately 50 % of confluency. The cells fixed with paraformaldehyde were used for immunostaining of PC [19, 20], pyruvate dehydrogenase (PDH)[20, 25], and glial fibrillary protein (GFAP) as already described. The affinity-purified antibodies against rabbit, human, or mouse IgG molecules were mixed in a blocking solution to a final ratio of 1:500 for each. The mixture was applied for 90 min. The Alexa Fluor 488 (Invitrogen, Thermo-Fisher) was bonded to anti-rabbit IgG molecules, while anti-human IgG molecules were covalently linked to TRITC (Invitrogen, Thermo-Fisher) and anti-mouse IgG with Alexa Fluor 633 (Invitrogen, Thermo-Fisher). The cell nuclei were visualized with DAPI (5 µg/ml), and stained cells were mounted with Fluoroshield (Sigma) to cover-glass. The negative controls were prepared by omitting the primary antibodies.

Preparation of human brain sections

Human brain tissue was obtained from Slovak Brain Bank (51-45739480-A0001, SK010922). The paraffin embedded cortex tissue was cut to prepare sections of 20 µm thickness. All experiments were monitored and approved by the Institutional Ethics Committee (Ethics Committee of Institute of Neuroimmunology, Slovak Academy of Sciences, Slovakia).

Immunohistochemistry

The immunofluorescent staining on the human brain sections was performed to visualize the presence of PC, PDH, GFAP, and neurofilament-200. The paraffin-embedded brain sections were stained after deparaffinization, dehydration, and antigen retrieval. The mixture of primary antibodies against PC and PDH was enriched

either with mouse anti-GFAP or anti-mouse against neurofilament-200 to perform the triple labelling. The primary antibodies were diluted to a final ratio of 1:250 each in TBS-T enriched with BSA to a final level of 2 mg/ml and applied at 4 °C overnight. After extensive washing, 3 x 10 min, the samples were incubated with a mixture of secondary antibodies consisting of goat anti-rabbit IgG conjugated with Alexa Fluor 488, anti-human IgG conjugated with TRITC, and anti-mouse IgG conjugated with Alexa Fluor 633 at RT for one hour. All secondary antibodies were diluted to a final ratio of 1:500, and their mixture was applied at RT for 1 h. The visualization of cell nuclei was performed by incubation with a solution of DAPI. The stained sections were mounted with Fluoroshield mounting medium.

Immunofluorescence analysis

The microscopic observation of the samples was done on the Zeiss Observer / LSM 710 confocal system (Carl Zeiss, Jena, Germany). The blue fluorescence of DAPI-stained nuclei was visualized by 405 nm laser and the proteins of interest were visualized using the laser set at 488 nm, 544 nm or 633 nm, depending on the fluorochrome coupled to secondary antibodies. All samples were scanned in Z-Stack mode with a 0.5 µm distance of individual optical sections. Zeiss Plan-Apochromat 20x / 0.8 M27 or 63 x oil objectives were used for all samples, with a resolution of 2048 pixels x 2048 pixels, with a pixel dwell set to 2.06 µsec. The resulting images were processed using Zeiss Zen Blue software.

Cellular viability test

MTT assay was performed to assess cellular viability [26]. Adherent astrocytes cells (K1884) seeded in triplicates in 96-well flat-bottomed plates at density 5 000 cells/well were preincubated in culture medium (93 % DMEM, 5 % FBS, 1 % N-2 supplement, 1 % penicillin/streptomycin) for 24 h. After preincubation, the refresh culture medium supplemented with either 3-chloro-1,2-dihydroxypropane (CDP) or oxamate to the final concentration range from 0.1 to 100 mM was added to 24- or 48-h incubation. After incubation, the media with CDP or oxamate were removed and culture medium supplemented with MTT was added, and incubation lasted for an additional 5 h. Subsequently, 100 µl of 10 % SDS solution was added to dissolve a

generated formazan. After the overnight incubation, the absorbance values at 540 nm were measured by Synergy H4 microplate reader (Bio Tek). 100 % survival, corresponded to the average absorbance value acquired for group of control cells. Pyruvate, citrate, 2-oxoglutarate, and malate were tested to revert the cytotoxic effect of CDP. The concentration of 10 mmol/l of one of the tested compounds was added to culture media supplemented with either 20 or 50 mmol/l CDP for two independent incubations lasting either 24 or 48 hours.

Estimation of pyruvate carboxylase and lactate dehydrogenase activity

PC enzymatic activity was estimated by modification of the method already described [27]. The reaction buffer (RB) for the assay consisted of 134 mM TRIS/HCl solution with a pH value set to 8.0 that was supplemented with 5 mM $MgCl_2$, 7 mM sodium pyruvate, 0.12 % (w/v) bovine serum albumin, 0.23 mM NADH, 0.05 mM acetyl coenzyme A, 5 units of malic dehydrogenase and 10 mU of pyruvate carboxylase. For the assay, into 290 µL of RB was added 30 µL of inhibitor solution in water with desired concentration, and subsequently, the reaction was started by the addition of 10 µL mixture of ATP (30 mM) and $KHCO_3$ (450 mM) in Tris (100 mM) solution with pH 8.0. The velocity of NADH oxidation was monitored at 340 nm and recorded by a Synergy H4 plate reader (BioTek) for 15 min at 37 °C and used to calculate the activity of PC by using the value of extinction coefficient for NADH equal to 6.22 $mM^{-1}.cm^{-1}$. The blank value was set when pyruvate carboxylase was omitted from RB. The control value of PC activity (100 % activity of PC) was estimated by omitting CDP and oxamate from the inhibitor solution.
The effect of PC inhibitors on LDH activity in vitro was estimated by modification of the method already described (Warren and Tipton 1974). Briefly, 300 µL of the reaction buffer 2 (RB2) that consisted of TBS pH 7.5 supplemented with 7 mM sodium pyruvate, 0.23 mM NADH, and 10 mU lactate dehydrogenase with was added 30 µL of inhibitor solution with desired concentration. The absorbance was monitored at 340 nm and recorded by a Synergy H4 plate reader (Bio Tek) for 15 min at 37 °C. Subsequently, the recorded change of absorbance was used to calculate the activity of LDH by using the value of extinction coefficient for NADH equal to 6.22 $mM^{-1}.cm^{-1}$. The blank value was established by omitting the lactate dehydrogenase

from RB2. Both compounds, CDP and oxamate were omitted from the reaction mixture to estimate the 100 %-age activity of LDH.

Statistical analysis

Mean ±SEM of three independent experiments are represented in the results. Differences among the tested groups were obtained by one-way analysis of variance with post hoc comparisons by Student-Newman-Keuls test. If the corresponding p values were lower than 0.05 between obtained data from different groups, the data sets were considered statistically significant. Indeed, the statistical analysis was achieved with the software InStat (GraphPad Software, USA).

Results

To assess PC expression in human astrocytes and the brain, we exploited the immune-based methods with rabbit serum-derived against purified PC [19]. The specificity of antiserum to specifically recognize the human homolog of PC was already rigorously tested and confirmed by several previous experiments [25, 28].

The Western blot analysis was performed (Fig. 1) to evaluate the presence of PC among the lysate proteins derived from the human brain cortex, cultured human normal astroglia cells (NHA), and cell line of differentiated astrocytes (K1884). All lysate samples were stained positively by Western blot analysis with used anti-PC serum (Fig. 1). The estimated relative mass of the appeared signal is approximately 125 kDa and corresponds to the deduced value of the molecular mass of PC. In addition, visualized protein bands exhibit a similar mass and specificity as the purified bovine PC protein. The obtained values of chemiluminescent signals for PC in different samples were normalized to the recorded chemiluminescent signal of GAPDH (Fig. 1).

The same antibodies were used to analyze the distribution of PC among cultured cells and the brain sections. A combination of primary antibodies anti-PC with secondary antibodies conjugated to Alexa Fluor 488 was used for immunofluorescence detection of PC expression in cultured K1884 cells (Fig. 2) and also among the cells in human cortex (Fig. 3, 4). In K1884 cells and the human cortex, the green signal was detected by fluorescence microscopy. The mitochondria were visualized by immunofluorescent staining of pyruvate dehydrogenase. The colocalization of both immunofluorescent signals for PC and PDH results to appearance of yellow dotty signal after merging (Fig. 3, 4). A combination of primary antibodies against astrocytic or neuronal marker, anti-GFAP (Fig. 3) or anti-neurofilament-200 (Fig. 4), respectively, with anti-PC was applied to identify the type of neural cells expressing PC in culture and also in human brain cortex sections. Negative controls were prepared by omitting the primary antibodies (Figs 2 – 4).

To assess the role of PC in the viability of astrocytes cells, we applied various concentrations of CDP or oxamate to culture media. CDP and oxamate are both

considered to be inhibitors of PC [29, 30]. The viability of cells was assessed by MTT test after incubation with the inhibitor for 24 or 48 h (Fig. 5, a). The results show that both compounds, CDP and oxamate, are capable to negatively affect the viability of the cultured astrocytes. CDP decreased the viability of the cells more potently and at a level of 50 mmol/l suppressed the cellular viability to approximately 60 % after 24-h incubation. Its effect was even more pronounced after 48-hour incubation when its level of 20 mmol/l initiated a drop of viability to approximately 50 %.

The capability of metabolites from the TCA cycle, namely 2-oxoglutarate, citrate, pyruvate, and malate, to revert the cytotoxic effect of CDP was tested by the MTT test (Fig.5, b). The K1884 cells were incubated in a culture medium supplemented with either one or combination of two TCA cycle metabolites in final level of 10 mmol/l in media containing also 20 mmol/l of CDP. Even though the supplementation of media with TCA cycle intermediates did not show any effect after 24-hour incubation (data not shown), prolong incubation for 48-hour reverted a cytotoxic effect of 20 mmol/l CDP (Fig. 5, b).

We tried to correlate the results of cytotoxic effect of CDP (Fig. 5, a) or oxamate (Fig. 5, b) on survival of cultured astrocytes with the potential of the both compounds to inhibit also PC activity *in vitro* (Fig. 6, a, b). Since, CDP and oxamate are structural analogues of pyruvate, we estimated their effect on activity of PC and LDH. The same levels of CDP inhibitors as were used in viability test, were used for the measurement of PC and LDH activity. All tested levels of CDP potently inhibited the enzymatic activities of both enzymes, PC and LDH (Fig. 6a).

Discussion

Despite the knowledge about the expression and presence of enzymatically active PC in the human brain [31], the cell-type-specific distribution of this enzyme had remained unrevealed [4]. Here we present the data that firmly assign the PC expression in human astrocytes either in cultures or *in situ*, and in addition, also show its presence among a small number of neurons in the human brain. Furthermore, we show that enzymatically active PC is vital for sustaining the viability of cultured astrocytes.

We used protein lysates derived from two types of cultured human astrocytes for immunoprobing detection of PC expression. The both, primary astroglia-rich culture derived from the adult brain (NHA) and human brain progenitor-derived astrocytes (K1884) express PC (Fig. 1). PC expression is ubiquitous among K1884 cells and is colocalized also in the subpopulation of GFAP-positive (Fig. 2) cells those are considered to be astroglia [32]. PC expression in cultured human astrocytes resembles its occurrence in cultured rodent astrocytes [19, 20, 33].

The Western blot analysis for PC expression among the proteins derived from human brain cortex (Fig. 1), together with the knowledge that enzymatic activity of PC is present in human brain [31] evoked the question about the putative glia-specific expression of PC in human brain. Indeed, immunofluorescent analysis of human brain cortex section confirmed the presence of PC among GFAP-positive, astroglial cells (Fig. 3). In addition, the signal for PC colocalized with neurofilament-200. Since neurofilament-200 is considered as a neuronal marker [34], our results indicate that some of the neurons in brain cortex are also bearing PC (Fig. 4). The expression of PC in neurons equips them with the tool for the potential enzymatic fixation of CO_2 on pyruvate. Although immunohistochemical staining is a valuable method to localize the presence of a gene expression product, it remains to be established to which extent PC expressed in neurons is also enzymatically active and contributes to neuronal metabolism. However, the results of the experiments performed on either cultured neural cells [35] or animals [36] suggest that carboxylation can also take place in neurons.

The primary antibodies, which we applied to visualize the presence of PC, were initially derived against bovine pyruvate carboxylase [19] and applied to detect PC in rodent glial cells [20]. Even there is a high degree of homology among the orthologues of the PC gene [37], we further confirmed the specificity of antibodies to recognize only PC out of the proteins present in lysates derived from a human brain or cultured astrocytes. The results of a series of experiments showed the capability of the antibodies to recognize only the biotin-containing protein with a molecular mass of 125 kDa. That confirms the specificity of used antibodies to recognize the human orthologue of PC [25, 28].

In astrocytes, the central role of PC has been supposed to be anaplerotic. The enzymatic prolongation of a pyruvate carbon skeleton to oxaloacetate provides the cells the ability to refill the level of TCA cycle intermediates [38]. The TCA cycle is central in both parts of cellular metabolism, intermediary and energetic. The intermediates of the TCA cycle are substrates for several cytosolic processes, including synthesis of lipids, reduction of cytosolic NADPH, and synthesis of non-essential amino acids [39]. Therefore, the inhibition of PC might slow down or prevent the continuation of several biochemical processes. Indeed, the inhibition of PC [30] by oxamate [40] or 3-chloro-1,2-propanediol (CDP) [29] negatively affects the survival of astrocytes (Fig. 5, a). Both compounds are structural analogues of pyruvate with the supposed capability to inhibit also lactate dehydrogenase [41] or aspartate transaminase [42].

To evaluate the effect of oxamate and CDP on lactate dehydrogenase and on pyruvate carboxylase activity was monitored *in vitro.* The correlation between CDP inhibition *in vitro* and in cellular viability are approximately at the same level, but also inhibition of LDH activity could have effect on cellular viability (Fig. 6, a). On the other hand, the compounds from TCA cycle reverted the lethal effect of PC inhibitor and increased the cellular viability. Therefore, we assume that the inhibition of an anaplerotic metabolism mediated by PC impacts cellular viability. Indeed, cytotoxic effect of CDP was suppressed by supplementation of culture media with citrate and 2-oxoglutarate (Fig. 5, b). This seems to be in agreement with molecular mechanism used in therapy of the patients with PC deficiency, when high doses of citrate provided to them is used to improve their metabolomic status [5].

Even oxamate potently inhibited the activities of the both enzymes, PC and LDH, when tested *in vitro* (Fig. 6, b), it did not affect the cellular viability on a large scale (Fig. 5, a). For this reason, we assume that the import of oxamate into mitochondrial compartment of cultured human astrocytes from extracellular milieu might be not sufficiently effective or oxamate could undergo structural changes those could affect its inhibitory effect.

The anaplerotic role of pyruvate carboxylase can significantly contribute to the brain metabolism by balancing its anabolic part with supplying the TCA cycle with oxaloacetate [4]. In this respect, pyruvate carboxylase responses for maintaining the metabolism of non-essential amino acids, e.g., glutamate [4, 33, 43–45], glutamine, and GABA; lipids [46], including cholesterol [47–49], and several other compounds [1, 2] those are essential for sustaining the physiological brain functions [23].

Conclusion

In summary, our experiments provide confirmed, that PC is expressed in cultured human astrocytes cells and also in astrocytes and in neurons cells of human brain. The anaplerotic activity of PC is necessary for viability of astrocytes cells line even in presence of another anaplerotic metabolite, glutamine. Indeed, the importance of anaplerosis facilitated by PC might be helpful in better understanding of cellular metabolism of these cells. Also, PC might be important in maintaining their growth and division, as well as in exchange of metabolites between astrocytes and neurons, for example citrate, cholesterol, etc. PC is considered as none neuron enzyme, but we provide evidence, that PC could be present in some neurons in human brain cortex. This knowledge might be helpful for better understanding of intercellular metabolism of human neurons and astrocytes and also in metabolomic cooperation between astrocytes and neurons.

Acknowledgements

The authors are very grateful to Bernd Hamprecht (University of Tuebingen, Germany) for the generous gift of anti-PC serum. Furthermore, we are grateful to Jana Harsányiová for her excellent technical help and valuable advice. This work was supported by projects: VEGA 1/0255/20, and by the Slovak Research and

Development Agency under the contract No. APVV-18-0088 and under the contract No. APVV-19-0033, and with the support of the Integrated Infrastructure Operational Program for the project: Systemic Public Research Infrastructure - Biobank for Cancer and Rare diseases, ITMS: 313011AFG5, co-financed by the European Regional Development Fund.

References

1. Inigo M, Deja S, Burgess SC (2021) Ins and Outs of the TCA Cycle: The Central Role of Anaplerosis. Annu Rev Nutr 41:19–47. https://doi.org/10.1146/annurev-nutr-120420-025558

2. Owen OE, Kalhan SC, Hanson RW (2002) The Key Role of Anaplerosis and Cataplerosis for Citric Acid Cycle Function. J Biol Chem 277:30409–30412. https://doi.org/10.1074/jbc.R200006200

3. Hassel B (2007) 3.1 Anaplerosis. In: Lajtha A, Gibson GE, Dienel GA (eds) Handbook of Neurochemistry and Molecular Neurobiology. Springer US, Boston, MA, pp 183–195

4. Schousboe A, Waagepetersen HS, Sonnewald U (2019) Astrocytic pyruvate carboxylation: Status after 35 years. J Neurosci Res 97:890–896. https://doi.org/10.1002/jnr.24402

5. Wang D, De Vivo D (1993) Pyruvate Carboxylase Deficiency. In: Adam MP, Ardinger HH, Pagon RA, et al (eds) GeneReviews®. University of Washington, Seattle, Seattle (WA)

6. Brun N, Robitaille Y, Grignon A, et al (1999) Pyruvate carboxylase deficiency: prenatal onset of ischemia-like brain lesions in two sibs with the acute neonatal form. Am J Med Genet 84:94–101

7. García-Cazorla A, Rabier D, Touati G, et al (2006) Pyruvate carboxylase deficiency: metabolic characteristics and new neurological aspects. Ann Neurol 59:121–127. https://doi.org/10.1002/ana.20709

8. Hidalgo J, Campoverde L, Ortiz JF, et al (2021) A Unique Case of Pyruvate Carboxylase Deficiency. Cureus 13:e15042. https://doi.org/10.7759/cureus.15042

9. Mhanni AA, Rockman-Greenberg C, Ryner L, Bunge M (2021) Prenatal onset of the neuroradiologic phenotype of pyruvate carboxylase deficiency due to homozygous PC c.1828G > A mutations. JIMD Rep 61:42–47. https://doi.org/10.1002/jmd2.12235

10. Mochel F, DeLonlay P, Touati G, et al (2005) Pyruvate carboxylase deficiency: clinical and biochemical response to anaplerotic diet therapy. Mol Genet Metab 84:305–312. https://doi.org/10.1016/j.ymgme.2004.09.007

11. Monnot S, Serre V, Chadefaux-Vekemans B, et al (2009) Structural insights on pathogenic effects of novel mutations causing pyruvate carboxylase deficiency. Hum Mutat 30:734–740. https://doi.org/10.1002/humu.20908

12. Schiff M, Levrat V, Acquaviva C, et al (2006) A case of pyruvate carboxylase deficiency with atypical clinical and neuroradiological presentation. Mol Genet Metab 87:175–177. https://doi.org/10.1016/j.ymgme.2005.10.007

13. Pardridge WM (1983) Brain metabolism: a perspective from the blood-brain barrier. Physiol Rev 63:1481–1535. https://doi.org/10.1152/physrev.1983.63.4.1481

14. Gruetter R, Novotny EJ, Boulware SD, et al (1994) Localized 13C NMR spectroscopy in the human brain of amino acid labeling from D-[1-13C]glucose. J Neurochem 63:1377–1385. https://doi.org/10.1046/j.1471-4159.1994.63041377.x

15. Hertz L, Chen Y (2017) Integration between Glycolysis and Glutamate-Glutamine Cycle Flux May Explain Preferential Glycolytic Increase during Brain Activation, Requiring Glutamate. Front Integr Neurosci 11:18. https://doi.org/10.3389/fnint.2017.00018

16. Gray LR, Tompkins SC, Taylor EB (2014) Regulation of pyruvate metabolism and human disease. Cell Mol Life Sci 71:2577–2604. https://doi.org/10.1007/s00018-013-1539-2

17. Shank RP, Bennett GS, Freytag SO, Campbell GL (1985) Pyruvate carboxylase: an astrocyte-specific enzyme implicated in the replenishment of amino acid neurotransmitter pools. Brain Res 329:364–367. https://doi.org/10.1016/0006-8993(85)90552-9

18. Shank RP, Leo GC, Zielke HR (1993) Cerebral metabolic compartmentation as revealed by nuclear magnetic resonance analysis of D-[1-13C]glucose metabolism. J Neurochem 61:315–323. https://doi.org/10.1111/j.1471-4159.1993.tb03570.x

19. Cesar M, Hamprecht B (1995) Immunocytochemical examination of neural rat and mouse primary cultures using monoclonal antibodies raised against pyruvate carboxylase. J Neurochem 64:2312–2318. https://doi.org/10.1046/j.1471-4159.1995.64052312.x

20. Murín R, Cesar M, Kowtharapu BS, et al (2009) Expression of pyruvate carboxylase in cultured oligodendroglial, microglial and ependymal cells. Neurochem Res 480–489

21. Amaral AI, Hadera MG, Tavares JM, et al (2016) Characterization of glucose-related metabolic pathways in differentiated rat oligodendrocyte lineage cells. Glia 64:21–34. https://doi.org/10.1002/glia.22900

22. Salganicoff L, Koeppe RE (1968) Subcellular Distribution of Pyruvate Carboxylase, Diphosphopyridine Nucleotide and Triphosphopyridine Nucleotide

Isocitrate Dehydrogenases, and Malate Enzyme in Rat Brain. J Biol Chem 243:3416–3420. https://doi.org/10.1016/S0021-9258(18)93324-7

23. Hassel B (2000) Carboxylation and anaplerosis in neurons and glia. Mol Neurobiol 22:21–40. https://doi.org/10.1385/MN:22:1-3:021

24. Bradford MM (1976) A rapid and sensitive method for the quantitation of microgram quantities of protein utilizing the principle of protein-dye binding. Anal Biochem 72:248–254. https://doi.org/10.1006/abio.1976.9999

25. Gondáš E, Kráľová Trančíková A, Majerčíková Z, et al (2021) Expression of pyruvate carboxylase in cultured human astrocytoma, glioblastoma and neuroblastoma cells. Gen Physiol Biophys 40:127–135. https://doi.org/10.4149/gpb_2021003

26. Mosmann T (1983) Rapid colorimetric assay for cellular growth and survival: application to proliferation and cytotoxicity assays. J Immunol Methods 65:55–63. https://doi.org/10.1016/0022-1759(83)90303-4

27. Warren GB, Tipton KF (1974) Pig liver pyruvate carboxylase. Purification, properties and cation specificity. Biochem J 139:297–310

28. Gondáš E, Kráľová Trančíková A, Dibdiaková K, et al (2023) Immunodetection of Pyruvate Carboxylase Expression in Human Astrocytomas, Glioblastomas, Oligodendrogliomas, and Meningiomas. Neurochem Res. https://doi.org/10.1007/s11064-023-03856-5

29. Doedens D, Ashmore J (1972) Inhibition of pyruvate carboxylase by chloropyruvic acid and related compounds. Biochem Pharmacol 21:1745–1751. https://doi.org/10.1016/0006-2952(72)90081-0

30. Zeczycki TN, Maurice MSt, Attwood PV (2010) Inhibitors of Pyruvate Carboxylase. Open Enzyme Inhib J 3:8–26. https://doi.org/10.2174/1874940201003010008

31. Atkin BM, Buist NRM, Utter MF, et al (1979) Pyruvate Carboxylase Deficiency and Lactic Acidosis in a Retarded Child without Leigh's Disease. Pediatr Res 13:109–116. https://doi.org/10.1203/00006450-197902000-00005

32. Zhang Z, Ma Z, Zou W, et al (2019) The Appropriate Marker for Astrocytes: Comparing the Distribution and Expression of Three Astrocytic Markers in Different Mouse Cerebral Regions. BioMed Res Int 2019:1–15. https://doi.org/10.1155/2019/9605265

33. Yu AC, Drejer J, Hertz L, Schousboe A (1983) Pyruvate carboxylase activity in primary cultures of astrocytes and neurons. J Neurochem 41:1484–1487. https://doi.org/10.1111/j.1471-4159.1983.tb00849.x

34. Yuan A, Rao MV, Veeranna, Nixon RA (2017) Neurofilaments and Neurofilament Proteins in Health and Disease. Cold Spring Harb Perspect Biol 9:a018309. https://doi.org/10.1101/cshperspect.a018309

35. Hassel B, Bråthe A (2000) Neuronal Pyruvate Carboxylation Supports Formation of Transmitter Glutamate. J Neurosci 20:1342–1347. https://doi.org/10.1523/JNEUROSCI.20-04-01342.2000

36. Hassel B, Bråthe A (2000) Cerebral metabolism of lactate in vivo: evidence for neuronal pyruvate carboxylation. J Cereb Blood Flow Metab Off J Int Soc Cereb Blood Flow Metab 20:327–336. https://doi.org/10.1097/00004647-200002000-00014

37. Jitrapakdee S, St Maurice M, Rayment I, et al (2008) Structure, mechanism and regulation of pyruvate carboxylase. Biochem J 413:369–387. https://doi.org/10.1042/BJ20080709

38. Cappel DA, Deja S, Duarte JAG, et al (2019) Pyruvate-Carboxylase-Mediated Anaplerosis Promotes Antioxidant Capacity by Sustaining TCA Cycle and Redox Metabolism in Liver. Cell Metab 29:1291-1305.e8. https://doi.org/10.1016/j.cmet.2019.03.014

39. Martínez-Reyes I, Chandel NS (2020) Mitochondrial TCA cycle metabolites control physiology and disease. Nat Commun 11:102. https://doi.org/10.1038/s41467-019-13668-3

40. Martin-Requero A, Ayuso MS, Parrilla R (1986) Interaction of oxamate with the gluconeogenic pathway in rat liver. Arch Biochem Biophys 246:114–127. https://doi.org/10.1016/0003-9861(86)90455-8

41. Zhai X, Yang Y, Wan J, et al (2013) Inhibition of LDH-A by oxamate induces G2/M arrest, apoptosis and increases radiosensitivity in nasopharyngeal carcinoma cells. Oncol Rep 30:2983–2991. https://doi.org/10.3892/or.2013.2735

42. Thornburg JM, Nelson KK, Clem BF, et al (2008) Targeting aspartate aminotransferase in breast cancer. Breast Cancer Res 10:R84. https://doi.org/10.1186/bcr2154

43. Oz G, Berkich DA, Henry P-G, et al (2004) Neuroglial metabolism in the awake rat brain: CO2 fixation increases with brain activity. J Neurosci Off J Soc Neurosci 24:11273–11279. https://doi.org/10.1523/JNEUROSCI.3564-04.2004

44. Andersen JV, Markussen KH, Jakobsen E, et al (2021) Glutamate metabolism and recycling at the excitatory synapse in health and neurodegeneration. Neuropharmacology 196:108719. https://doi.org/10.1016/j.neuropharm.2021.108719

45. Andersen JV, Christensen SK, Westi EW, et al (2021) Deficient astrocyte metabolism impairs glutamine synthesis and neurotransmitter homeostasis in a mouse model of Alzheimer's disease. Neurobiol Dis 148:105198. https://doi.org/10.1016/j.nbd.2020.105198

46. Barber CN, Raben DM (2019) Lipid Metabolism Crosstalk in the Brain: Glia and Neurons. Front Cell Neurosci 13:212. https://doi.org/10.3389/fncel.2019.00212

47. Zhang J, Liu Q (2015) Cholesterol metabolism and homeostasis in the brain. Protein Cell 6:254–264. https://doi.org/10.1007/s13238-014-0131-3

48. Jin U, Park SJ, Park SM (2019) Cholesterol Metabolism in the Brain and Its Association with Parkinson's Disease. Exp Neurobiol 28:554–567. https://doi.org/10.5607/en.2019.28.5.554

49. Dietschy JM, Turley SD (2001) Cholesterol metabolism in the brain. Curr Opin Lipidol 12:105–112. https://doi.org/10.1097/00041433-200104000-00003

Figure 1. The immunoblotting analysis of the pyruvate carboxylase (PC) expression in cultured human astrocytes (K1884, NHA) and in lysate from human cortex (cortex). Western blot analysis was used to estimate the presence of PC and GAPDH among the proteins in cell lysates. Purified pyruvate carboxylase (rec. PC) was used as positive control.

Figure 2. Immunofluorescence detection of the presence of pyruvate carboxylase (PC), and glial fibrillary acidic protein (GFAP) in human astrocytes (K1884). The expression of pyruvate carboxylase, and glial fibrillary acidic protein in the cells was immunofluorescently labeled with primary anti-PC rabbit, and anti-GFAP mouse polyclonal antibodies followed by affinity-purified secondary antibodies anti-rabbit conjugated to Alexa Fluor 488 (green), and anti-mouse conjugated with Alexa Fluor 633 (red). DAPI intercalating fluorochrome (DAPI; blue) was used to visualize of cell nuclei. The merged views of the PC, GFAP and DAPI are represented in the last column (merge; orange). Negative control was made by omitting primary antibodies (negative control). The scale bars represent 20 μm and in bottom merge represent 10 μm.

Figure 3. Immunohistochemical detection of the presence of pyruvate carboxylase (PC), pyruvate dehydrogenase (PDH) and glial fibrillary acidic protein (GFAP) in human brain section. The expression of PC, PDH and GFAP in the cells was immunofluorescently labeled with primary anti-PC rabbit polyclonal antibodies, anti-PDH human polyclonal antibodies and anti-GFAP mouse monoclonal antibodies followed by affinity-purified anti-rabbit secondary antibodies conjugated to Alexa Fluor 488 (green), anti-human secondary antibodies conjugated to TRITC (orange) and anti-mouse secondary antibodies conjugated to Alexa Fluor 633 (red). Nuclei were visualized using DAPI intercalating fluorochrome (DAPI; blue). The merged views of the PC, PDH, GFAP and DAPI are represented in merge (yellow). Negative control was made by omitting primary antibodies (negative control). The scale bars represent 20 μm and in bottom merge represents 10 μm.

Figure 4. Immunohistochemical detection of the presence of pyruvate carboxylase (PC), pyruvate dehydrogenase (PDH) and neurofilament-200 (neurofilament) in human brain cortex section. The expression of PC, PDH and neurofilament-200 in

the cells was immunofluorescently labeled with primary anti-PC rabbit polyclonal antibodies, anti-PDH human polyclonal antibodies and anti-neurofilament mouse monoclonal antibodies followed by affinity-purified anti-rabbit secondary antibodies conjugated to Alexa Fluor 488 (green), anti-human secondary antibodies conjugated to TRITC (orange) and anti-mouse secondary antibodies conjugated to Alexa Fluor 633 (red). Nuclei were visualized using DAPI intercalating fluorochrome (DAPI; blue). The merged views of the PC, PDH, neurofilament-200 and DAPI are represented in merge (yellow). Negative control was made by omitting primary antibodies (negative control). The scale bars represent 20 μm and in bottom merge represent 10 μm.

Figure 5. The effect of CDP or oxamate on viability of human astrocytes (K1884) assessed by MTT test. a) Incubation of K1884 cells with culture media supplemented with CDP (○, □) or oxamate (●, ■) for either 24 (○, ●) or 48 (□, ■) hours. b) The potential of reverse cytotoxic effect of 20mmol/l CDP during 48h incubation with 10 mmol/l concentration of 2-oxoglutarate (2-OG), citrate (Cit), pyruvate (Pyr), and malate (Mal) was estimated by MTT-test. As 100 % survival was used the average of absorbances from group incubated with culture media without addition of CDP. ** $p < 0,01$; *** $p < 0,001$.

Figure 6. The effect of CDP or oxamate on inhibition of PC and LDH activity *in vitro* by measuring the absorbance of NADH at 340 nm. Monitoring of PC and LDH activity inhibition by spectrophotometric measurement of NADH formation at concentrations from 1 to 100 mM of CDP (a) or at concentration from 1 to 10 mM of oxamate (b). 100% group represent the measurement of activity without influence of CDP or oxamate.

Figure 1

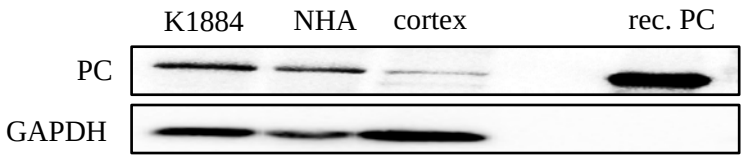

Figure 2

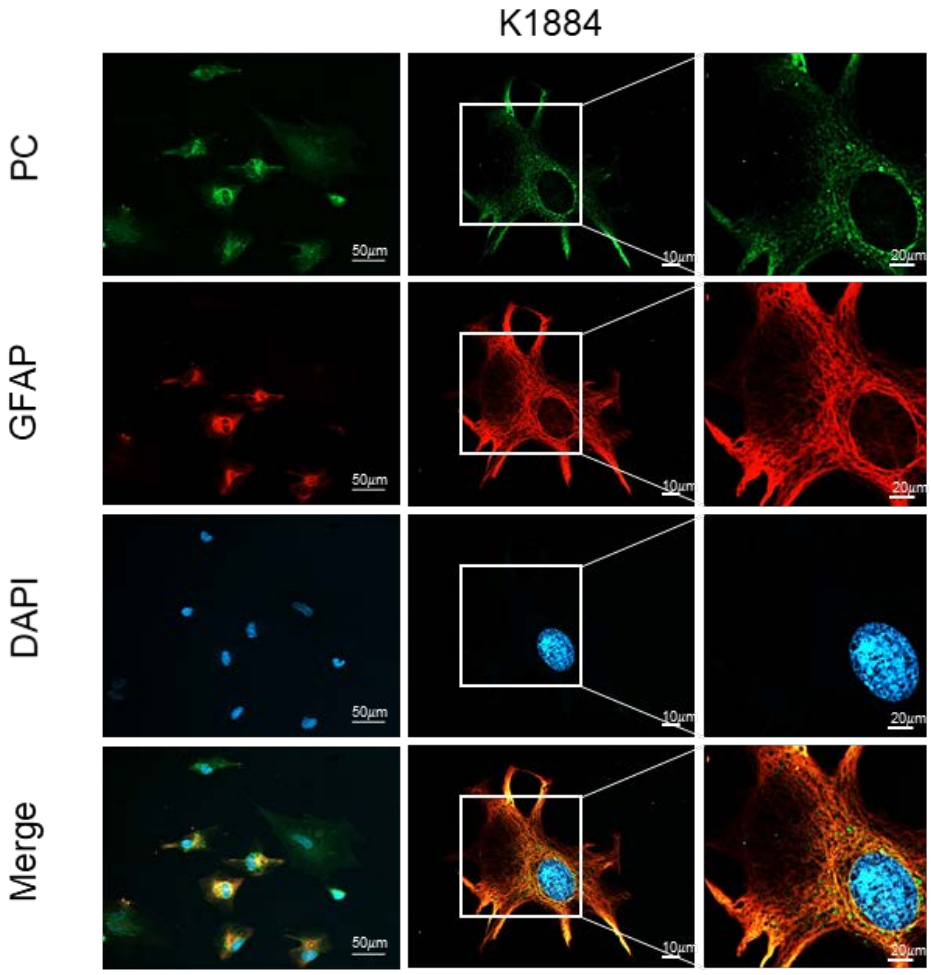

Figure 3

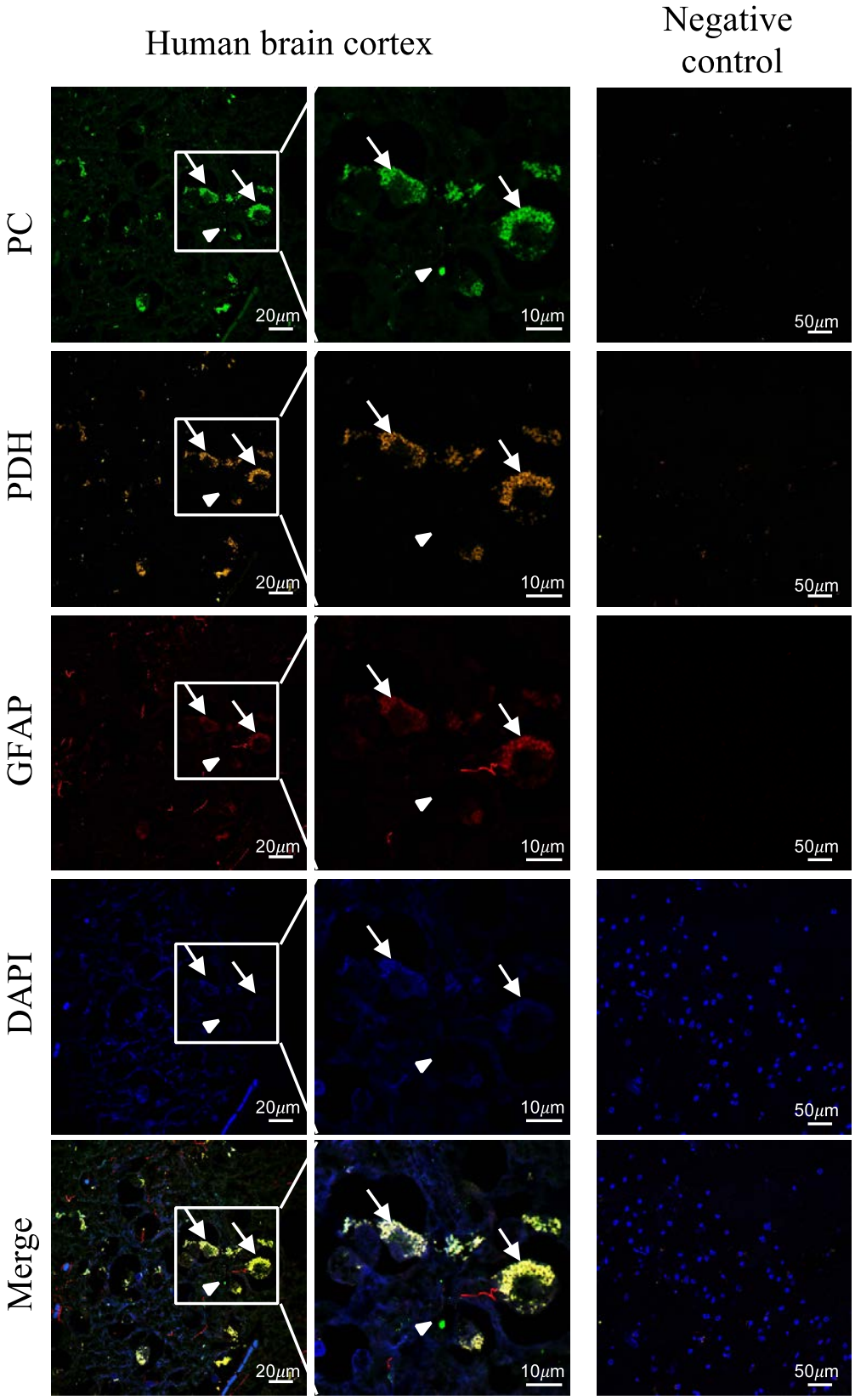
Human brain cortex
Negative control
PC
PDH
GFAP
DAPI
Merge
20μm
10μm
50μm

Figure 4

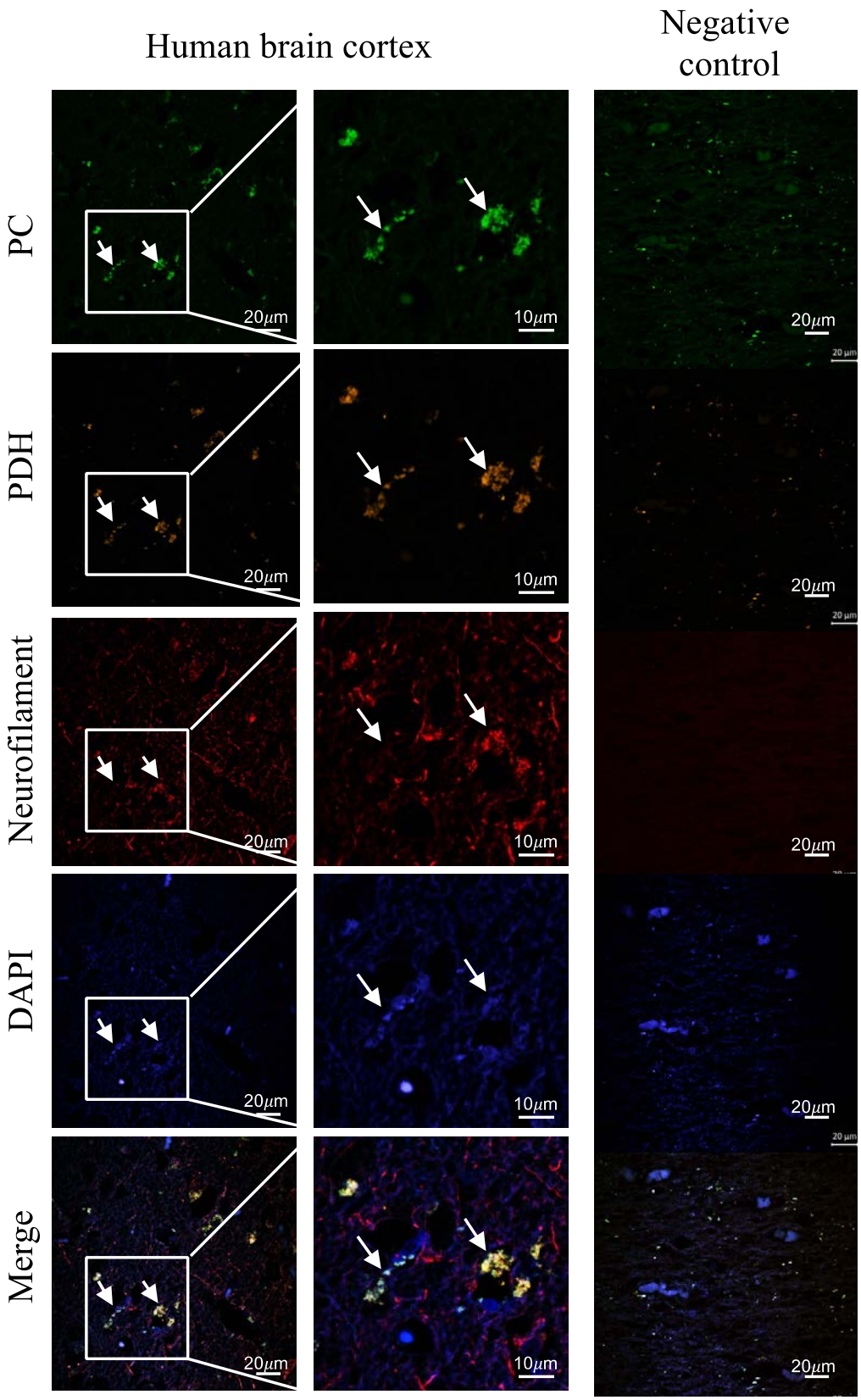
Human brain cortex
Negative control
PC
PDH
Neurofilament
DAPI
Merge
20μm
10μm

Figure 5.

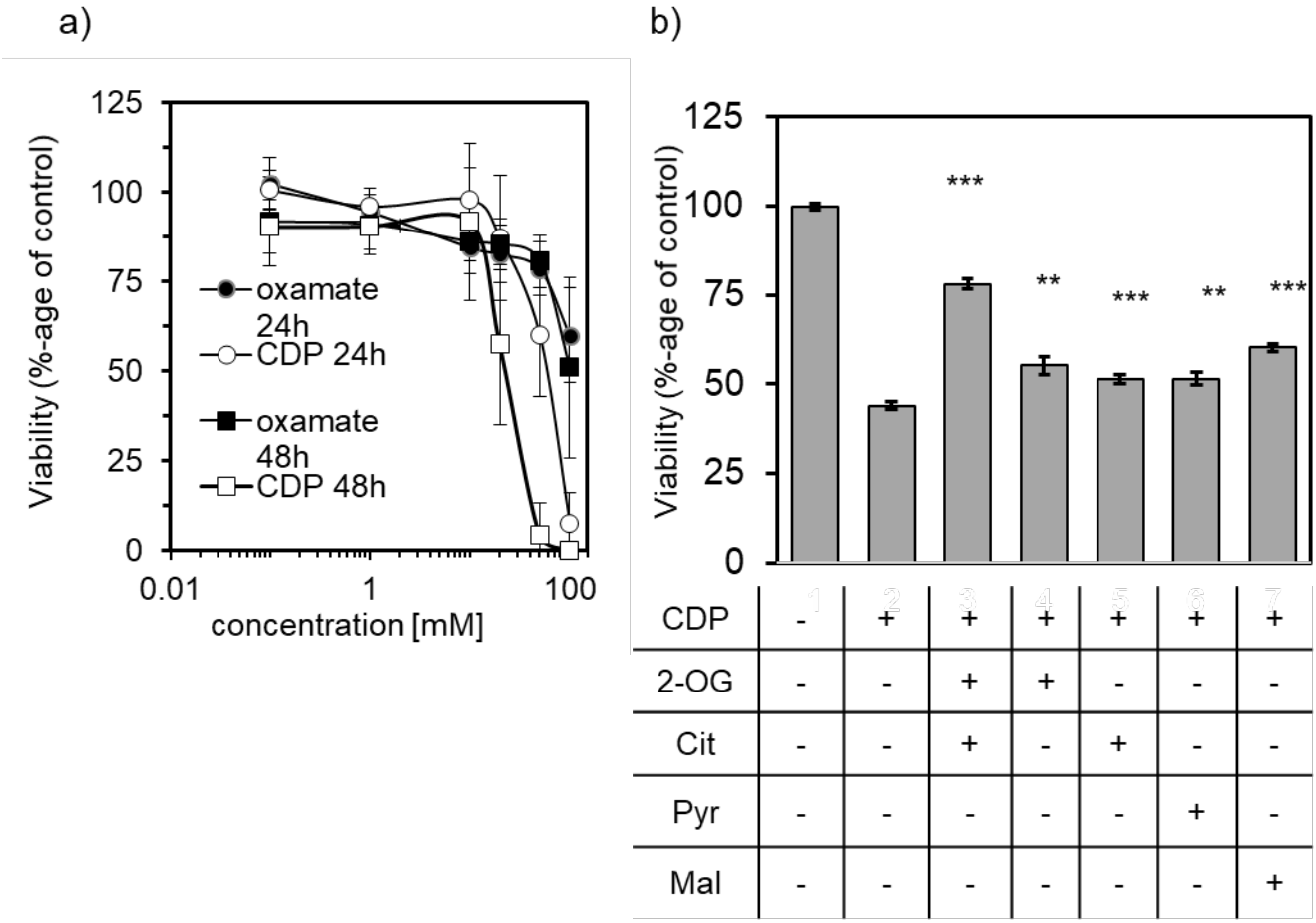
a)
b)
Viability (%-age of control)
125
100
75
50
25
0
0.01
1
100
concentration [mM]
oxamate 24h
CDP 24h
oxamate 48h
CDP 48h
***
**
***
**
***
1
2
3
4
5
6
7
CDP - + + + + + +
2-OG - - + + - - -
Cit - - + - + - -
Pyr - - - - - + -
Mal - - - - - - +

Figure 6

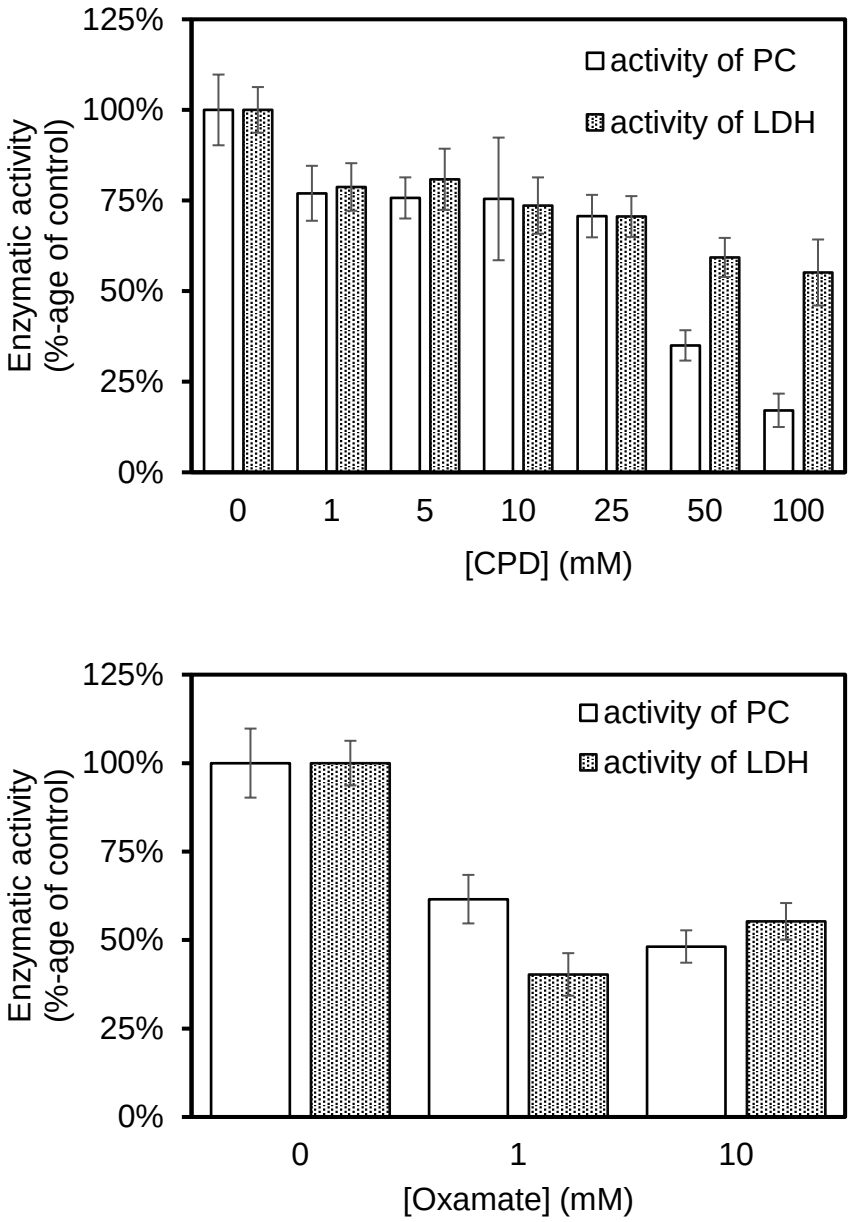
125%
100%
75%
50%
25%
0%
Enzymatic activity
(%-age of control)
activity of PC
activity of LDH
0
1
5
10
25
50
100
[CPD] (mM)
125%
100%
75%
50%
25%
0%
Enzymatic activity
(%-age of control)
activity of PC
activity of LDH
0
1
10
[Oxamate] (mM)